

Reduction of the primary donor P700 of photosystem I during steady-state photosynthesis under low light in *Arabidopsis*

Michito Tsuyama · Yoshichika Kobayashi

Received: 17 April 2008 / Accepted: 6 October 2008 / Published online: 31 October 2008
© Springer Science+Business Media B.V. 2008

Abstract During steady-state photosynthesis in low-light, 830-nm absorption (A_{830}) by leaves was close to that in darkness in *Arabidopsis*, indicating that the primary donor P700 in the reaction center of photosystem I (PSI) was in reduced form. However, P700 was not fully oxidized by a saturating light pulse, suggesting the presence of a population of PSI centers with reduced P700 that remains thermodynamically stable during the application of the saturating light pulse (i.e., reduced-inactive P700). To substantiate this, the effects of methyl viologen (MV) and far-red light on P700 oxidation by the saturating light pulse were analyzed, and the cumulative effects of repetitive application of the saturating light pulse on photosynthesis were analyzed using a mutant *crr2-2* with impaired PSI cyclic electron flow. We concluded that the reduced-inactive P700 in low-light as revealed by saturating light pulse indicates limitations of electron flow at the PSI acceptor side.

Keywords Absorption at 830 nm · Acceptor limitation · Chlorophyll fluorescence · Electron flow · Photosynthesis · Photosystem I

Abbreviations

A_{830}	Leaf absorption at 830 nm
Chl	Chlorophyll
F_m and F_m'	Maximum fluorescence level in the dark- and light-adapted leaf, respectively
F_s and F_o	Steady state- and minimum-fluorescence level, respectively

FR	Far-red light
MV	Methyl viologen
P700	Primary donor pigment in the reaction center of PSI

Introduction

During photosynthesis in higher plants, electrons are transported from PSII, via plastoquinone (PQ), the cytochrome b_6/f complex (Cyt b_6/f), and plastocyanin (PC), to PSI and beyond NADP. Electron transport from PQ to Cyt b_6/f couples to the proton translocation across the thylakoid membrane. The resulting proton gradient (ΔpH) across the thylakoid membrane provides the proton with the motive force to drive the synthesis of ATP, which together with NADPH sustains much of the metabolism in the stroma. To match the metabolic requirements, electron flow is regulated. First, behind the increased ΔpH , excess excitation energy in PSII is dissipated as heat via a radiationless process. Second, the increased ΔpH inhibits, by feedback action, electron flow during plastoquinol oxidation at Cyt b_6/f . This inhibition, known as photosynthetic control, causes oxidation of P700 (Harbinson et al. 1990; Laisk et al. 2005). Oxidized P700 quenches excitation energy as heat (Nuijs et al. 1986).

Most of the P700 stays reduced during steady-state photosynthesis in low-light. This indicates that photosynthetic control does not function as above and that oxidized P700 is completely re-reduced by electrons transported from PSII. A proportion of the reduced form of P700, which can be estimated from leaf absorbance at 830 nm, has been treated as an indicator of the efficiency of electron transport in PSI (for review, Baker et al. 2007). This is based on the assumption that all reduced forms of P700 are

M. Tsuyama (✉) · Y. Kobayashi
Department of Agriculture, Kyushu University,
6-10-1 Hakozaki, Higashi-ku, Fukuoka 812-8581, Japan
e-mail: mtsuyama@agr.kyushu-u.ac.jp

capable of undergoing charge separation and donating electrons to downstream acceptors. Indeed, in the isolated reaction center of PSI, the quantum yield of charge separation is close to one (Hiyama 1985). However, a proportion of reduced P700 always does not indicate the efficiency of PSI. Harbinson and Hedley (1993) showed that, during the early stages of photosynthetic induction in high-light, a lack of regeneration of NADP produces a pool of reduced P700 which limits the overall rate of electron transport in the thylakoid. This was confirmed by Klughammer and Schreiber (1994), who used saturating light pulses to quantify the pool of reduced and photochemically-inactive P700. That is, in the presence of limited electron flow at the acceptor side of PSI, P700 oxidation by saturating light pulse is partly inhibited, revealing the lower PSI efficiency than that expected from the proportion of reduced P700.

The extent of acceptor limitation of electron flow in PSI is determined by regeneration of oxidized PSI electron acceptors (Harbinson and Hedley 1993; Klughammer and Schreiber 1994). Antisense potato plants with lower amounts of ferredoxin (Fd) showed severe PSI acceptor limitation even in low-light (Holtgreffe et al. 2003). Also, taking the decrease in oxidizability of P700 by far-red light in leaves pre-illuminated with strong light as an indicator of PSI acceptor limitation, its occurrence was confirmed in some tropical plants from a neotropical forest (e.g., *Anacardium excelsum*, *Piper carrilloanum*) (Barth et al. 2001) and in sun-exposed leaves from sun plants (e.g., *Quercus glauca*) (Endo et al. 2005). In these cases, pre-illumination with strong light was stimulated, due to PSI acceptor limitation by a lack of NADP⁺, the cyclic electron transport around PSI (Barth et al. 2001), and/or charge recombination within PSI (Endo et al. 2005). Further, in cucumber, a chilling-sensitive plant, PSI acceptor limitation was initially present at low temperatures and in low-light, whereas finally leading to oxidative destruction of the iron–sulfur clusters in PSI (Sonoike et al. 1995).

Extreme variations can be found in the literature describing the redox state of the NADP system in the stroma (Takahama et al. 1981; Dietz and Heber 1984; Rebeille and Hatch 1986; Cerovic et al. 1993). For example, the NADP system is not much reduced even in high-light in sunflower (Laisk et al. 1991) and in pea (Foyer et al. 1992), whereas it is significantly reduced even in the dark and in low-light in spinach (Heineke et al. 1991) and in barley (Forti et al. 2003). On the other hand, Laisk et al. (2005) showed that the photosynthetic control (originated from increasing counter-pressure to proton release during PQH₂ oxidation at Cyt *b₆f*) is present not only in high-light but also in low-light. They attributed the low-light down-regulation of Cyt *b₆f* to regulatory H⁺ backpressure generated from O₂-related mechanisms, such as O₂ photo-reduction, on the basis of the

observation that down-regulation was removed at low O₂. Also, Oja et al. (2003) found that P700 stayed reduced at limited-light intensities, which suggests that reduction of the PSI acceptor side increases with increasing light. However, the result is based on the assumption of a free redox equilibration between PC and P700, i.e., PC should be partly oxidized while P700 remains reduced, and increasing evidence is accumulating that no free redox equilibration in the high potential chain from cytochrome *f* (cyt *f*) in the Cyt *b₆f* to P700 occurs (Kirchhoff et al. 2004; Joliot and Joliot 2005).

In this study, we focus on regulation of electron flow in PSI in low-light in *Arabidopsis*. Analyses of P700 redox changes induced by a saturating light pulse suggested limitation of electron flow at the acceptor side of PSI in low-light. Behind the PSI acceptor limitation, the saturating light pulse was assumed to induce charge recombination in PSI, followed by production of reduced-inactive P700 that results from a proportion of the reduced P700 not being oxidized by the saturating light pulse.

Materials and methods

Arabidopsis thaliana wild type (ecotype Columbia *gll*) and a mutant *crr2-2* (*chlororespiratory reduction*) (Hashimoto et al. 2003) were grown in soil under growth chamber conditions (60 μmol photons m⁻² s⁻¹, 50% RH, 10 h-light/14 h-dark cycles, 23°C) for 8–10 weeks. Representative mature leaves of healthy appearance were selected from vigorous individuals. For treatment with methyl viologen (MV, 1,1'-dimethyl-4,4'-dipyridinium dichloride), plants were sprayed with 100 μM MV in 0.25% Tween 20 and kept in darkness for at least 4 h to infiltrate the MV into the leaves.

Modulated chlorophyll fluorescence was measured using a PAM 101 fluorometer (H. Walz, Germany). For determining minimal (F_o) and maximal (F_m) fluorescence, leaves were kept in darkness for at least 1 h prior to use. F_o was induced by red-modulated measuring light of PFD of <0.5 μmol photons m⁻² s⁻¹. F_m and F_m' (maximal fluorescence in the light) were determined by applying approximately 1.0 s pulse of saturating white light (ca. 8,000 μmol photons m⁻² s⁻¹). The non-photochemical quenching coefficient of chlorophyll fluorescence (NPQ), the maximum quantum yield of PSII (F_v/F_m), and the quantum yield of PSII in the light (ΦPSII) were determined as (F_m - F_m')/F_m', (F_m - F_o)/F_m, and (F_m' - F_s)/F_m', respectively. F_v, F_o, and F_s are variable, minimum, and steady-state fluorescence, respectively (Genty et al. 1989).

To monitor the redox state of P700, leaf absorbance around 830 nm was measured using the same system as for the measurement of chlorophyll fluorescence (a PAM 101 fluorometer) equipped with a dual wavelength

(810/860 nm) emitter–detector unit (ED-P700DW, H. Waltz, Effeltrich, Germany) (Klughammer and Schreiber 1994). The proportion of oxidized P700, reduced-inactive P700, and reduced-active (i.e., the quantum yield of PSI) were determined as $A_{830}/A_{830\max}$, $(A_{830\max} - A_{830\max}')/A_{830\max}$, and $(A_{830\max}' - A_{830})/A_{830\max}$, respectively (Klughammer and Schreiber 1994). A_{830} , $A_{830\max}$, and $A_{830\max}'$, respectively, undergo absorption at 830 nm under illumination with actinic light, that is induced by the pulse of saturating light (as used for the measurements of chlorophyll fluorescence) given on top of far-red light (36 W m^{-2}) and that induced by the saturating pulse given in a steady state attained by actinic light. Far-red light ($>720 \text{ nm}$) was obtained by passing light from the halogen light source (KL 1500, Schott, Germany) through a long-pass filter. According to Klughammer and Schreiber (1994), to assure detection of $A_{830\max}$ and $A_{830\max}'$, an electric shutter system (EMJ, Fukuoka, Japan) was employed, which makes it possible to provide the saturating light pulse within 1 ms while blocking illumination of far-red or actinic light. Data were collected using an A/D converter (Powerlab 200, AD Instruments, Australia) at a sampling rate of 1 ms per point.

Results

Non-oxidized and photochemically-inactive P700 in low-light

Figure 1a and b show an example of changes in chlorophyll fluorescence and leaf absorbance at 830 nm (A_{830}) measured in low-light ($60 \mu\text{mol photons m}^{-2} \text{ s}^{-1}$) in normal air conditions in a dark-adapted leaf of the wild type. About 30 min of illumination was sufficient to reach a steady state. Under these conditions, non-photochemical quenching of chlorophyll fluorescence did not develop, as indicated by the level of F_m' being almost the same as that of F_m (Fig. 1a). Steady-state A_{830} was similar to that at the beginning of the measurements in darkness (Fig. 1b), indicating that P700 was in the non-oxidized (reduced) form. Application of a pulse of saturating light caused P700 oxidation (as indicated by an increase in A_{830}). However, this P700 oxidation was incomplete and the level was markedly smaller than its maximum ($A_{830\max}$) which was established by the saturating light pulse in combination with far-red light. This result indicates that photochemistry was not possible in some PSI reaction centers. Figure 1c and d summarize the results of the measurements carried out at a range of irradiances. In low-light of $60 \mu\text{mol photons m}^{-2} \text{ s}^{-1}$, the relative amount of oxidized P700 was approximately 5%. The quantum yield of PSI (ΦPSI), as determined from the increase in A_{830} due to the saturating

light, was approximately 0.7, almost identical to that of PSII (ΦPSII). The remaining approximately 25% can be assigned to the relative proportion of PSI centers with P700 in photochemically inactive form (reduced-inactive P700), which was determined from the difference between $A_{830\max}$ and $A_{830\max}'$. This proportion decreased, with increasing irradiance, to almost zero at a PFD of $800 \mu\text{mol photons m}^{-2} \text{ s}^{-1}$, and then increased to approximately 15% at $1,770 \mu\text{mol photons m}^{-2} \text{ s}^{-1}$. In short, the proportion of reduced-inactive P700 was high in low- and in high-light.

Effects of O_2 removal on reduced-inactive P700 in low-light

After reaching a steady state in low-light, oxygen was removed from the air (Fig. 1a, b). This did not significantly alter A_{830} , indicating that P700 remained in non-oxidized form (Fig. 1b). Removal of O_2 had less effect on the quantum yield of PSII (Fig. 1c), although the F_m' level declined slightly in O_2 -free air as compared to air (Fig. 1a). Pulse-induced rises of A_{830} increased in O_2 -free air (Fig. 1b), indicating an increase in the quantum yield of PSI and associated decrease of reduced-inactive P700 (Fig. 1d). This effect of O_2 removal was not observed in high-light (Fig. 1d). Figure 1e shows changes in A_{830} during the pulse on an enlarged timescale. In air (Curve 3), A_{830} initially increased (i.e., P700 was oxidized) upon illumination by the saturating pulse, followed by a sudden decrease (i.e., re-reduction of P700). On the other hand, in O_2 -free air, A_{830} increased more than in air and was largely stable during the pulse (Curve 4).

The response of A_{830} to the saturating light pulse was tested in the dark (Curves 1 and 2 in Fig. 1e). Under these conditions, FNR (ferredoxin-NADP reductase) is expected to be inactivated (Nikolaeva 2001). The drop in A_{830} after its initial increase was more marked than in the light and A_{830} declined below the dark level (compare Curves 1 and 3). This result indicates that limitation of electron flow at the acceptor side of PSI enhanced P700 re-reduction during the saturating light pulse. Further, successive illumination of the saturating light pulse hindered the initial increase of A_{830} (compare Curves 1 and 2), suggesting that P700 oxidation by the pulse depends on the redox state of the electron acceptors in PSI, since pre-illumination by the saturating light pulse will result in a reduction of electron acceptors in PSI, such as the iron–sulfur acceptors F_X , F_A , and F_B . It is therefore possible to assume that the accumulation of reduced-inactive P700 in air in low-light (Fig. 1d, Curve 3 in Fig. 1e) was also due to limitation of electron flow at the acceptor side of PSI. Further, this PSI acceptor limitation is suggested to be linked to a form of oxygen-related metabolism, since reduced-inactive P700 was largely eliminated in O_2 -free air (Fig. 1d, Curve 4 in Fig. 1e).

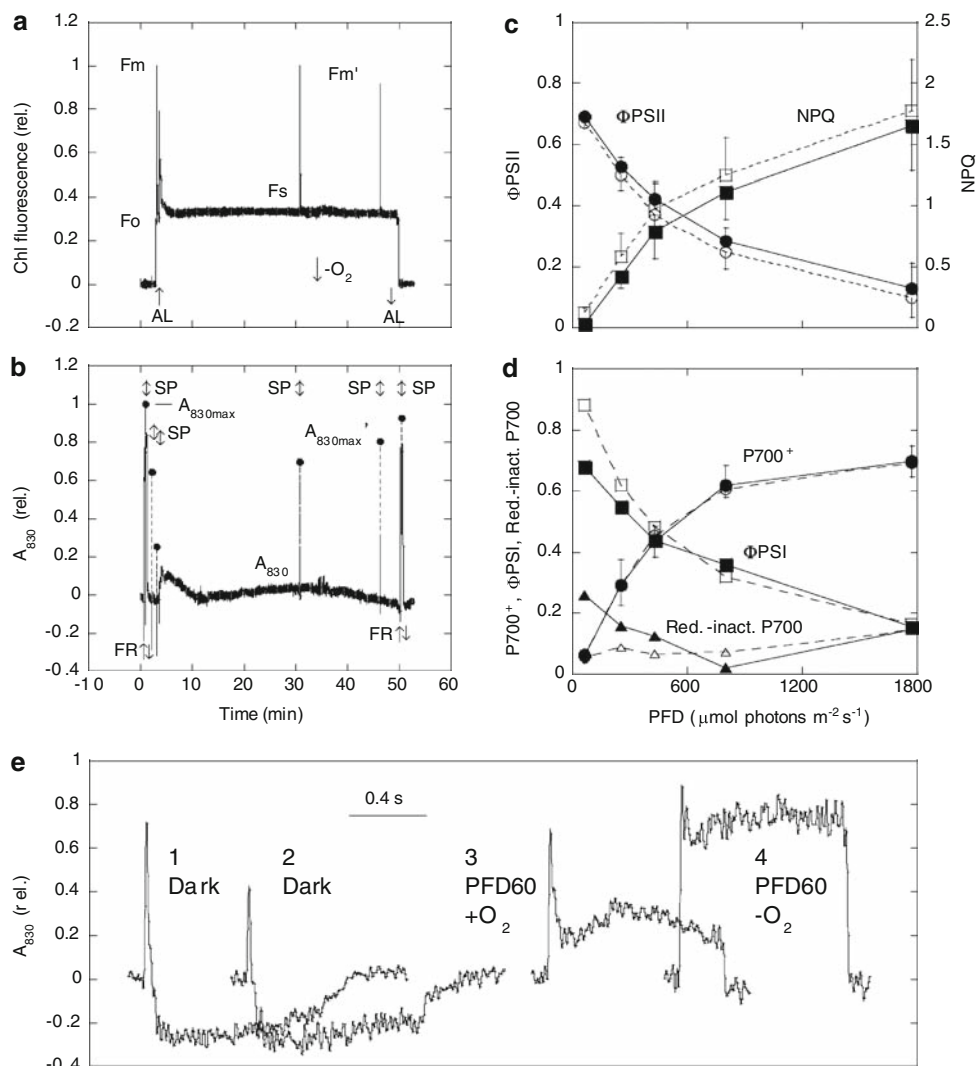


Fig. 1 Non-oxidized P700 in steady-state photosynthesis in low-light. **a** Kinetics of chlorophyll fluorescence and **b** leaf absorbance at 830 nm in an *Arabidopsis* leaf. The leaf was first illuminated with far-red light (FR) and a pulse of saturating light (SP) was applied to detect the maximum absorbance at 830 nm ($A_{830\max}$). After switching off the far-red light, the saturating light pulse was applied successively to observe P700 oxidation in the dark. Photosynthesis was initiated in air under actinic light (AL) of PFD of $60 \mu\text{mol photons m}^{-2} \text{s}^{-1}$, and approximately 30 min after the onset of the AL, the saturating light pulse was applied to detect the maximum fluorescence (F_m') and 830-nm absorbance ($A_{830\max}'$) in the light. The O_2 was then removed from the air. About 15 min later, the saturating light pulse was applied. **c** The quantum yield of PSII (ΦPSII ; ●, ○), non-photochemical quenching coefficient of chlorophyll fluorescence (NPQ; ■, □) and **d** proportion of oxidized P700 (P700^+ ; ●, ○),

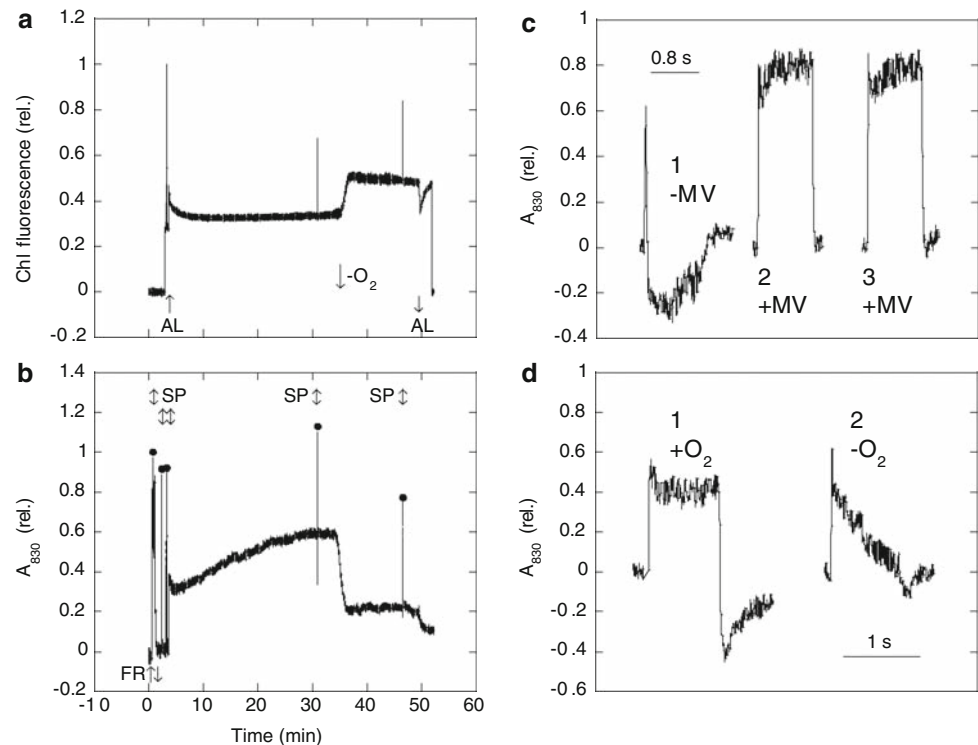
reduced-active P700 (i.e., the quantum yield of PSI ΦPSI , ■, □), and reduced-inactive P700 (▲, △) as a function of PFD in air (closed symbols) and O_2 -free air (open symbols). The quantum yield of PSI was determined from an initial peak of 830-nm absorbance increase (i.e., P700 oxidation) upon illumination of the saturating pulse as shown in **e**. Bars are mean \pm S.D. for at least five experiments. **e** Changes in 830-nm absorbance during application of the saturating light pulse. As shown in **b**, the 830-nm absorbance increase (i.e., P700 oxidation) was induced by the saturating light pulse in the dark successively (Curves 1 and 2) and during steady-state photosynthesis in air (Curve 3) and in O_2 -free air (Curve 4). Data from at least five experiments, in which the 830-nm absorbance was recorded at a sampling rate of 1 ms/point and normalized to $A_{830\max}$, were averaged

It should be noted that ferredoxin (Fd) reduction decreases A_{830} (Oja et al. 2003; Harbinson and Hedley 1989; Klughammer and Schreiber 1991), which may explain the drop of A_{830} below dark level (Curves 1 and 2 in Fig. 1e). This is supported by the following experiments, which were done in the presence of MV, where such an excessive drop of A_{830} was not observed.

Effects of methyl viologen on the accumulation on reduced-inactive P700

Figure 2 shows an example of the results of the same experiments as in Fig. 1 in a leaf treated with MV. MV accepts electrons from PSI, turning into a MV radical which reacts rapidly with dioxygen (Hiyama and Ke 1971;

Fig. 2 Effects of methyl viologen on PSI acceptor limitation in low-light. **a** Kinetics of chlorophyll fluorescence and **b** leaf absorbance at 830 nm in the presence of 100 μ M methyl viologen. Experimental procedures are as in Fig. 1a and b. **c, d** Changes in 830-nm absorbance during application of the saturating light pulse. The 830-nm absorbance increase (i.e., P700 oxidation) was induced by the saturating light pulse in the dark in the absence of MV as a control line (**c**, Curve 1) or in the presence of 100 μ M MV successively (**c**, Curves 2 and 3) and during steady-state photosynthesis in air (**d**, Curve 1) and in O_2 -free air (**d**, Curve 2). Data from at least five experiments were averaged, as in Fig. 1e



Golbeck and Cornelius 1986). In the control leaves sprayed with detergent solution only (0.25% Tween 20; Curve 1 in Fig. 2c), P700 was largely re-reduced during illumination by the saturating light pulse given in the dark, as illustrated in Fig. 1e (Curve 1). In leaves treated with MV (100 μ M), P700 was mostly oxidized and the oxidation level remained stable during the application of the saturating light pulse (Curve 2 in Fig. 2c). In addition, the saturating light pulse given consecutively did not affect the responses of P700 redox state to the pulse (Curve 3), in contrast to the observation in the absence of MV (Curves 1 and 2 in Fig. 1e). These results indicate that electron donation to oxygen via MV relieved the limitation of electron flow at the acceptor side of PSI caused by the dark-inactivation of FNR.

At low-light (60 μ mol photons $m^{-2} s^{-1}$), the oxidized form of P700 increased sharply upon exposure to the actinic light and thereafter the oxidation level changed less (Fig. 2b). Under these conditions, less reduced-inactive P700 was detected. However, as a result of removing oxygen from the air, the P700 oxidation decreased and reduced-inactive P700 appeared. These results indicate that MV-mediated electron flow to oxygen caused the P700 oxidation and prevented an accumulation of reduced-inactive P700 in air, confirming that limitation of electron flow at the acceptor side of PSI in air in low-light was responsible for the accumulation of reduced-inactive P700 (Fig. 1d, Curve 3 in Fig. 1e). Table 1 summarizes the results of this experiment. Asada et al. (1990) previously

Table 1 Quantum yield of PSII, proportion of oxidized P700, reduced-active P700 (quantum yield of PSI), and reduced-inactive P700 in the presence of methyl viologen before and after removal of oxygen from the air

	Φ_{PSII}	P700 ⁺	Φ_{PSI}	Reduced-inactive P700
Air	0.51 (0.02)	0.42 (0.08)	0.55	0.03
O_2 -free air	0.42 (0.1)	0.16 (0.03)	0.61	0.23

Experimental conditions are as in Fig. 2a and b. The quantum yield of PSI was determined, as in Fig. 1d, from an initial peak of 830-nm absorbance increase (P700 oxidation) upon illumination with the saturating pulse (Fig. 2c, d). Mean values (\pm S.D.) for at least five experiments are shown

showed, in intact or broken spinach chloroplasts, that electron flow to MV is inhibited under anaerobic conditions. Our observation that the quantum yield of PSII declined due to the removal of oxygen (Fig. 2a, Table 1) supports their results. This may explain the increases in steady-state fluorescence (F_s) resulting from O_2 removal in the presence of MV (Fig. 2a), the time course of which matched the P700⁺ reduction (Fig. 2b). Both the changes in fluorescence and P700 redox state are consistent with the accumulation of electrons at the acceptor side of PSI.

In the presence of MV, the P700 oxidation level during the saturating light pulse was stable both in the dark (Curves 2 and 3 in Fig. 2c) and in the light (Curve 1 in Fig. 2d), except in O_2 -free air in the light (Curve 2 in Fig. 2d). These results suggest that, in accordance with the results obtained in the absence of MV (Curves 1–4 in

Fig. 1e), the PSI acceptor limitation is manifested by P700 re-reduction during the saturating light pulse. This indicator was utilized in the analyses below.

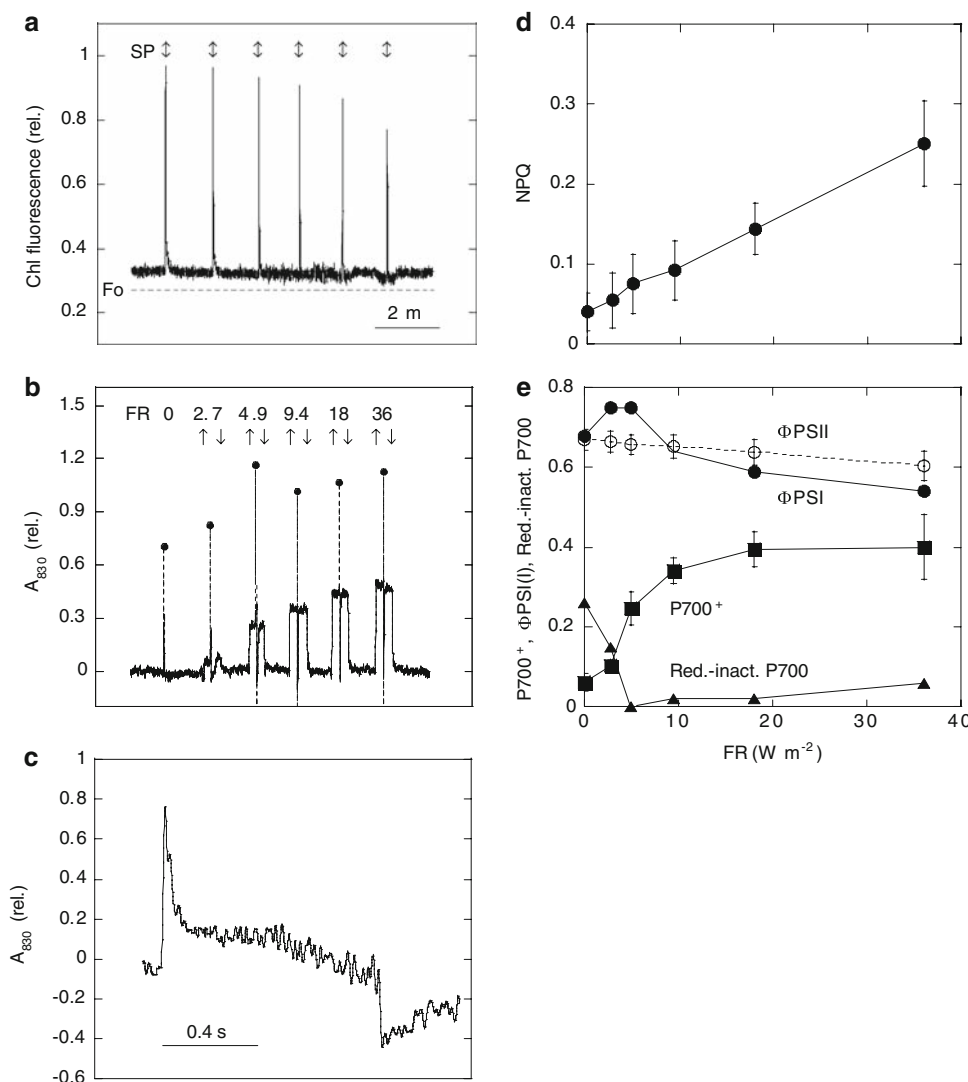
Effects of far-red light on the accumulation of reduced-inactive P700

Far-red light excites PSI preferentially. Therefore, it must be possible to oxidize the portion of reduced-inactive P700. Figures 3a and b show the results of an experiment in which far-red light at various intensities was provided to a leaf photosynthesizing in low-light ($60 \mu\text{mol photons m}^{-2} \text{s}^{-1}$). As expected, by increasing the intensity of far-red light up to 4.9 W m^{-2} , i.e., the range where the PSII quantum yield was almost unaffected (Fig. 3a, e), the proportion of reduced-inactive P700 decreased to zero (Fig. 3b, e). On the other hand, the P700 redox state was not stable and severe P700 re-reduction was observed during the application of a saturating light pulse (Fig. 3c). This indicates that

the PSI acceptor limitation remained under far-red light which was sufficient to remove all reduced-inactive P700.

In the above experiment, although weak far-red light had almost no effect on chlorophyll fluorescence, strong far-red light decreased F_m' considerably (Fig. 3a). The resulting non-photochemical quenching of chlorophyll fluorescence increased linearly with increasing intensity of far-red light (Fig. 3d). Electron donation from PSII to PSI would be determined by excitation of PSII by background white light even under strong far-red light. This is supported by the quantum yield PSII being relatively insensitive to far-red illumination (Fig. 3e). On the other hand, the P700 redox state was sensitive to far-red light (Fig. 3b, e). The P700 oxidation level reached a plateau at 20 W m^{-2} and about 40% of P700 was oxidized. This remarkable oxidation of P700 was accompanied by a decline of the quantum yield of PSI below that of PSII. Since an oxidized form of P700 quenches excitation energy as heat and produces no charge separation, the result implies that PSI was over-excited by

Fig. 3 Effects of far-red light on PSI acceptor limitation in low-light. **a** Kinetics of chlorophyll fluorescence and **b** leaf absorbance at 830 nm at different intensities of far-red light provided under background white light. During steady-state photosynthesis under background white light of PFD of approximately $60 \mu\text{mol photons m}^{-2} \text{s}^{-1}$, a pulse of saturating light was applied in the absence of far-red light and subsequently in the presence of far-red light with different irradiances of 2.7, 4.9, 9.4, 18.0, and 36.0 W m^{-2} . **c** Changes in 830-nm absorbance during application of the saturating light pulse under the far-red light of 4.9 W m^{-2} . Data from at least five experiments were averaged as in Fig. 1e. **d** Non-photochemical quenching coefficient (NPQ), **e** the quantum yield of PSII (Φ_{PSII} , \circ), proportion of oxidized P700 (P700^+ , \blacksquare), reduced-active P700 (i.e., the quantum yield of PSI Φ_{PSI} , \bullet), and reduced-inactive P700 (\blacktriangle) as a function of far-red light intensity. Experimental conditions are as in **a** and **b**. The quantum yield of PSI was determined, as in Fig. 1d. Bars are mean \pm S.D. for at least five experiments



the strong far-red light, which might result, via an imbalance between the activities of both photosystems, in the observed increase in NPQ (Fig. 3a, d). It should also be noted that $A_{830\max}'$ relative to $A_{830\max}$ sometimes exceeded one in the presence of far-red light (Fig. 3b). The A_{830} signal includes the contribution of PC oxidation (Oja et al. 2003; Harbinson and Hedley 1989; Klughammer and Schreiber 1991), which might be responsible for the excessive value in $A_{830\max}'/A_{830\max}$. There is thus a possibility that reduced-inactive P700 disappeared at a higher far-red light intensity than that presented (i.e., 4.9 W m^{-2} , Fig. 3b, e).

Repetitive application of the saturation light pulse in low-light

To further substantiate the limitation of electron flow at the acceptor side of PSI in low-light, here we dissected the issue and investigated whether the application of a saturating light pulse makes it possible to detect the PSI acceptor limitation. In the experiment shown in Fig. 4a, the saturating light pulse was repetitively applied to a leaf once a minute for long periods (17 to 18 h) in low-light. This repetitive application resulted in a progressive decline in the quantum yield of PSII (Φ_{PSII}) with the elapse of time or the number of saturating pulses applied. However, the maximum quantum yield of PSII, determined in the dark by $F_v/F_m = (F_m - F_o)/F_m$, showed less changed: the value remained at approximately 0.8, even after switching off the low-light. This result indicates that the decline of Φ_{PSII} in the light was due to damage to components other than PSII.

Therefore, in this experiment, the saturating pulse was used to determine the PSII quantum yield (i.e., Φ_{PSII} and F_v/F_m) on the one hand, but at the same time it caused damage to photosynthesis when being applied to leaves many times.

The same experiment was done with *Arabidopsis* mutant *crr2-2* (Hashimoto et al. 2003) (Fig. 4a), in which the electron recycling around PSI from NADPH to PQ is impaired due to a defect in the expression of a subunit of the NAD(P)H dehydrogenase (NDH) complex (reviewed by Shikanai 2007). *crr2-2* is therefore prone to suffer PSI acceptor limitation. While the PSII quantum yield in the dark (F_v/F_m) was less affected, the decline of Φ_{PSII} in the light was more pronounced in *crr2-2* than in the wild type. This result suggests the involvement of the PSI acceptor limitation in the decline of Φ_{PSII} . As to the inhibition site, the decline of Φ_{PSII} in the light was accompanied by a decrease in relative oxidizability of P700, determined after the repetitive application of a saturating pulse (Fig. 4b), suggesting that the decline in Φ_{PSII} was due to PSI inhibition. Collectively, the results suggest that the repetitive illumination of the saturating pulse reveals, as damage to PSI, the limitation of electron flow at the acceptor side of PSI.

Discussion

Acceptor limitation of electron flow in PSI in low-light

There was a population of reduced-inactive P700 in low- and in high-light (Fig. 1d). P700 is oxidized by donor-side

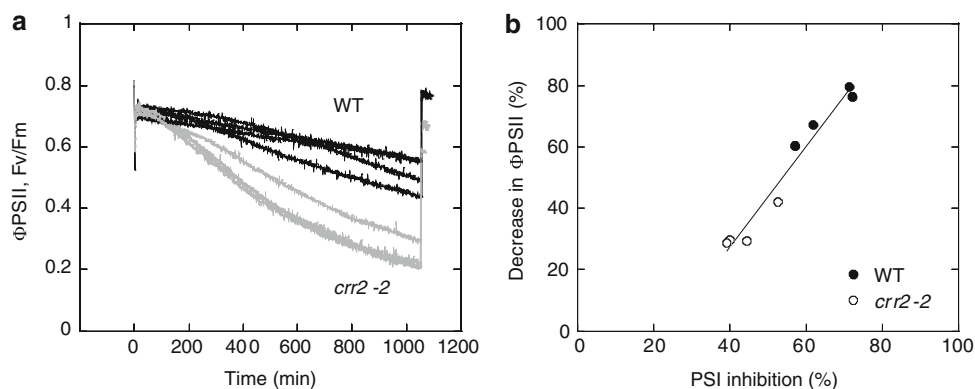


Fig. 4 Repetitive application of the saturating light pulse. **a** Changes in the quantum yield of PSII. Dark-adapted leaves of the *Arabidopsis* wild type (*black*) and mutant *crr2-2* (*gray*) were first illuminated with a saturating light pulse to determine the maximum quantum yield of PSII in the dark, $F_v/F_m = (F_m - F_o)/F_m$. The leaves were then illuminated with low-light of approximately $60 \mu\text{mol photons m}^{-2} \text{ s}^{-1}$ while applying the saturating light pulse every minute to determine the PSII quantum yield in the light, $\Phi_{\text{PSII}} = (F_m' - F_s)/F_m'$. Finally, the leaves were again placed in the dark and the saturating pulses were applied at the same interval to determine the PSII quantum yield in the dark (F_v/F_m). Results from different

specimens are shown. **b** Relationship between the degree of PSI inhibition and decline of the PSII quantum yield in the light Φ_{PSII} . The PSI inhibition was estimated from the ratio of $A_{830\max, \text{ before}}/A_{830\max, \text{ after}}$, where $A_{830\max, \text{ before}}$ and $A_{830\max, \text{ after}}$ are 830-nm absorbance induced by strong far-red light (36 W m^{-2}) before and after the repetitive (approximately 1,070 times) exposure of the saturating light pulse, respectively. The decline of the PSII quantum yield in the light was determined from the ratio of Φ_{PSII} obtained during the initial steady state in low-light to that obtained under the same light conditions but after repetitive (approximately 1,050 times) exposure of the saturating light pulse. Wild type (WT), ●; *crr2-2*, ○

limitation as a result of the photosynthetic control at Cyt *b₆f* (Harbinson et al. 1990; Laisk et al. 2005). However, P700 oxidation was not detected in low-light (60 $\mu\text{mol photons m}^{-2} \text{s}^{-1}$) and reached a plateau in high-light (1,770 $\mu\text{mol photons m}^{-2} \text{s}^{-1}$) (Fig. 1d). This result indicates that reduced-inactive P700 appears when no or no further photosynthetic control takes place out of the range of photosynthetic control. On the other hand, there is a possibility of involvement of the different activation status of the Calvin cycle enzymes (Sage 1990). The proportion of active versus inactive enzymes is low in low-light, which thereby might explain the presence of reduced-inactive P700 in low-light. However, this is unlikely because at high CO_2 , where rubisco activation decreases similarly (Sage 1990), the PSI acceptor limitation (as manifested by P700 re-reduction during the saturation light pulse) was in contrary relieved (data not shown).

The redox status of electron acceptors in the stroma has been extensively studied. The reported proportion of NADPH (% of NADPH plus NADP) in the dark and in high-light were respectively: in leaves, approximately 35 and 50% in pea (Foyer et al. 1992), 19 and 33% in spinach (Heineke et al. 1991); in protoplasts, 47 and 27% in *Avena sativa* (Hampp et al. 1984); in chloroplasts, 50 and <50% in spinach (Takahama et al. 1981), no data and 64% in spinach (Dietz and Heber 1984). In C_4 maize mesophyll chloroplasts, in which the Calvin–Benson cycle is absent, the values in the dark and in the light were, respectively, approximately 9–15 and 19–32% (Usuda 1988), and 20–25 and 65% (Rebeille and Hatch 1986). On the other hand, although little attention has been paid to the proportion in low-light, Takahama et al. (1981) showed that in spinach chloroplasts, the NADP system was reduced in low-light (NADPH proportion of 85%) to a greater degree than in high-light (75%) during photosynthetic induction. Similarly, in barley leaves, the NADP level declined to less than half of the dark level during steady state in very low-light of 10 $\mu\text{mol photons m}^{-2} \text{s}^{-1}$ (Forti et al. 2003). Also, Laisk et al. (1991) showed in sunflower leaves that the proportion of NADPH showed less change after transition from low- to high-light: the NADPH ratio in the former was approximately 39% and in the latter 44%, respectively, except during photosynthetic oscillation. It appears difficult to generalize the redox state of the NADP system from these early data, but the NADP system is likely to be partly reduced, even in low-light, to an extent comparable to that in high-light. On the other hand, as discussed previously in terms of the mass action ratio of the PGA (3-phosphoglycerate) reducing system (Takahama et al. 1981; Dietz and Heber 1984; Cerovic et al. 1993; Oja et al. 2003), the redox state of the NADP system is controlled by the ratio of PGA to DHAP (dihydroxyacetone phosphate) and by the phosphorylation potential $[\text{ATP}]/[\text{ADP}][\text{Pi}]$. Further, there

is considerable freedom of adjustment among those three components, i.e., $[\text{NADPH}]/[\text{NADP}]$, $[\text{PGA}]/[\text{DHAP}]$, and $[\text{ATP}]/[\text{ADP}][\text{Pi}]$. It is therefore possible to assume that the reduction level of NADP system rises even in low-light due to a low PGA/DHAP ratio and low phosphorylation potential. The observed population of reduced-inactive P700 in low-light (Fig. 1d) may be produced in such situations. The reason that O_2 removal, eliminated reduced inactive P700 (Fig. 1) likely relates to the NADPH/ATP consumption ratio in the Calvin cycle, since the PSI acceptor limitation also depended upon CO_2 concentration (data not shown).

Mechanisms involved in the generation of reduced-inactive P700

As discussed previously (Golding and Johnson 2003), the question arises as to the nature of this reduced-inactive P700. They observed an increase in the proportion of reduced-inactive P700 under stressed conditions (low CO_2 and drought) and proposed that charge recombination or back reaction in PSI is responsible for the occurrence of reduced-inactive P700. Under conditions where reducing power accumulates in the stroma, electron acceptors in PSI, such as F_X , F_A , and F_B are reduced. Forward electron transfer reactions compete with back reactions, which are possible between radical pairs of P700^+ and any reduced acceptors in PSI (for review, Brettel and Leibl 2001). Therefore, within a time scale of some 10 ns (for $\text{P700}^+\text{A}_0^-$) to <100 ms (for $\text{P700}^+\text{F}_\text{A}^-/\text{F}_\text{B}^-$), radical pairs may undergo a charge recombination reaction and then P700^+ may return, partly via a triplet excited state, to a singlet ground state while dissipating the excess excitation energy as heat (Brettel and Leibl 2001; Shinkarev et al. 2002). The charge recombination will not favor accumulation of P700^+ as a whole and will consequently increase the proportion of reduced P700 which behaves as if insensitive to the saturating light pulse (similar to populations of reduced-inactive P700 in the present study).

The question remains as to whether charge recombination in PSI occurs in low-light. The kinetics of the P700 redox state during the saturating pulse changed in a complex manner in air, characterized by two large decreasing phases indicating P700^+ reduction (Curve 3 in Fig. 1e). However, both reduction phases were almost absent in O_2 -free air (Curve 4 in Fig. 1e). It is therefore important to note that the saturating light pulse alone was insufficient to cause P700 re-reduction during the pulse (Curve 3 in Fig. 1e) and that the P700 re-reduction was a product of combination of the saturating light pulse and the background limitation of electron flow at the acceptor-stromal side of PSI. It therefore seems best to conclude that, in air in low-light, the saturating light pulse caused charge

recombination and then resulted in P700 re-reduction during the saturating light pulse. However, the detected reduced-inactive P700 reflects the P700 population that does not have any access or link to electron acceptors in the steady state in low-light.

PSI acceptor limitation in low-light as revealed by saturating pulse-induced charge recombination in PSI

After dark adaptation, a fast P700 oxidation completed in approximately 100 ms was followed by a large and constitutive re-reduction of P700⁺ during illumination by the saturating pulse (Curve 1 in Fig. 1e). Forward electron flow from PSI is impossible in dark adapted-leaves due to dark inactivation of ferredoxin-NADP reductase (Nikolaeva 2001). Talts et al. (2007) reported that under these conditions, PSI cyclic electron flow can occur at a quantum yield of close to one if far-red light is present. Joliot and Joliot (2002) also showed that upon illumination of dark-adapted leaves with saturating light, PSI cyclic electron flow was induced at a rate similar to the maximum rate of linear electron transport. In addition, in the PSI reaction centers involved in this cyclic electron flow, the iron-sulfur acceptors F_A and F_B were reduced, inducing the charge recombination process between radical pair P700⁺F_x⁻ (Joliot et al. 2004). In our experiments performed in the presence of MV (Curves 2 and 3 in Fig. 2c), P700 largely stayed in the oxidized form during the saturating pulse; and the second pulse did not alter this change. Methyl viologen accepts electrons from F_A/F_B and inhibits the charge recombination reaction between P700⁺A₀⁻/A₁⁻ (Takahashi and Katoh 1984). Therefore, the effects of MV strongly suggest the involvement of charge recombination in the re-reduction of P700 during the saturating pulse in the absence of MV (Curves 1 and 2 in Fig. 1e). On the other hand, in the presence of MV, P700 was largely oxidized and reduced-inactive P700 was not detected in air in low-light (Fig. 2b), but subsequent O₂ removal decreased the P700 oxidation level and produced reduced-inactive P700 (Fig. 2b). These results collectively suggest that the reduced-inactive P700 in air in low-light in the absence of MV (Fig. 1b) was due to accumulation of electrons by the saturating light pulse either at the site of F_A/F_B, where MV accepts electrons, or at more upstream acceptors, like A₀, A₁, or F_x.

The electron donors to P700 (PC, Rieske Fe-S and cyt *f* in the Cyt *b₆f*.) will be highly reduced at the light-limited range of photosynthesis. Under these conditions, as mentioned previously (Siebke et al. 1997; Johnson 2005; Baker et al. 2007), the saturating pulse itself may induce a reduction of electron acceptors in the stroma by transferring electrons which reside in those high potential donors. This

may result in an overestimation of a proportion of reduced-inactive P700. In an attempt to avoid this possibility and to determine the quantum yield of PSI, Siebke et al. (1997) used a brief (0.5 s) pulse of far-red light to illuminate a leaf immediately before providing the saturating pulse of white light. The far-red pulse was intended to deplete the electrons residing in the intersystem electron carriers. In our experiments shown in Fig. 3, the pulse of saturating white light was provided under conditions where illumination of far-red was present and P700 was partially pre-oxidized. The thus obtained P700 oxidation by the saturating light pulse indeed increased somewhat under relatively weak far-red light of less than approximately 5 W m⁻² (Fig. 3e). However, in this situation, P700 re-reduction was still observed during the saturating pulse (Fig. 3c), as in the absence of far-red light (Curve 3 in Fig. 1e). This is likely to be attributable to charge recombination in PSI by the saturating pulse due to limitation of electron flow at the acceptor side of PSI. We therefore concluded that the fraction of reduced-inactive P700 in low-light was not due to electrons residing in the high potential chain but due to a lack of electron acceptors in the stroma.

In Fig. 4, the repetitive exposure of saturating light pulse resulted in the selective inhibition of PSI, which was enhanced in the *crr2-2* mutant. In spite of the impairment in the NADPH-dependent electron recycling around PSI, no phenotype has been reported in short-term photosynthesis in *crr2-2* (Hashimoto et al. 2003; Rumeau et al. 2005). For this reason, we tried to find cumulative effects of the saturating light pulse to gain insight into the PSI acceptor limitation in low-light. Consequently, we encountered PSI inhibition, but not PSII (Fig. 4b). This was an unexpected result, since PSII, in particular the D1 protein, is generally the main target for light stress (Aro et al. 1993). However, this specific PSI inhibition appears to be consistent with the proposed charge recombination in PSI induced by the saturating pulse applied in low-light (Figs. 1–3).

The result showing that PSI inhibition was more severe in *crr2-2* than in the wild type suggests that PSI acceptor limitation is responsible for the PSI inhibition (Fig. 4b). This PSI inhibition must be primarily dependent on the saturating light pulse, but combined illumination of the saturating light pulse and low-light appeared to be necessary to induce apparent PSI inhibition, as presented in Fig. 4. The reason for this is not known, but likely relates to factors, such as active oxygen scavenging and another Fd-dependent path for PSI cyclic electron flow. The results in Fig. 4 indicate that the saturating light pulse at least allows us to approach, probably via the PSI charge recombination, the PSI acceptor limitation in low-light. The physiological relevance of the PSI acceptor limitation in low-light requires further experiments.

In summary, our data indicates that PSI acceptor limitation occurs during steady-state photosynthesis not only in high-light but also in low-light. The PSI acceptor limitation in low-light is realized by the reduced inactive P700 that is induced by the application of a saturating light pulse, probably due to charge recombination in PSI. The fraction of reduced-inactive P700 in low-light reflects adjustment of electron flow in PSI to downstream limitation in the stroma.

Acknowledgments We thank Dr. Toshiharu Shikanai (Kyoto University) for helpful discussions and suggestions. This work was supported by a Grant-in-aid for Young Scientists B (18780117) from MEXT to Michito Tsuyama, for Young Scientists from Kyushu University to Michito Tsuyama, and for Scientific Research on Priority Areas (16085206) from MEXT to Toshiharu Shikanai.

References

- Aro EM, Virgin I, Andersson B (1993) Photoinhibition of photosystem II. Inactivation, protein damage and turnover. *Biochim Biophys Acta* 1143:113–134. doi:[10.1016/0005-2728\(93\)90134-2](https://doi.org/10.1016/0005-2728(93)90134-2)
- Asada K, Neubauer C, Heber U, Schreiber U (1990) Methyl viologen-dependent cyclic electron transport in spinach chloroplasts in the absence of oxygen. *Plant Cell Physiol* 31:557–564
- Baker NR, Harbinson J, Kramer DM (2007) Determining the limitations and regulation of photosynthetic energy transduction in leaves. *Plant Cell Environ* 30:1107–1125. doi:[10.1111/j.1365-3040.2007.01680.x](https://doi.org/10.1111/j.1365-3040.2007.01680.x)
- Barth C, Krause GH, Winter K (2001) Responses of photosystem I compared with photosystem II to high-light stress in tropical shade and sun leaves. *Plant Cell Environ* 24:163–176. doi:[10.1111/j.1365-3040.2001.00673.x](https://doi.org/10.1111/j.1365-3040.2001.00673.x)
- Brettel K, Leibl W (2001) Electron transfer in photosystem I. *Biochim Biophys Acta* 1507:100–114. doi:[10.1016/S0005-2728\(01\)00202-X](https://doi.org/10.1016/S0005-2728(01)00202-X)
- Cerovic ZG, Bergher M, Goulas Y, Tosti S, Moya I (1993) Simultaneous measurement of changes in red and blue fluorescence in illuminated isolated chloroplasts and leaf pieces: the contribution of NADPH to the blue fluorescence signal. *Photosynth Res* 36:193–204. doi:[10.1007/BF00033038](https://doi.org/10.1007/BF00033038)
- Dietz KJ, Heber U (1984) Rate-limiting factors in leaf photosynthesis. I. Carbon fluxes in the Calvin cycle. *Biochim Biophys Acta* 767:432–443. doi:[10.1016/0005-2728\(84\)90041-0](https://doi.org/10.1016/0005-2728(84)90041-0)
- Endo T, Kawase D, Sato F (2005) Stromal over-reduction by high-light stress as measured by decreases in P700 oxidation by far-red light and its physiological relevance. *Plant Cell Physiol* 46:775–781. doi:[10.1093/pcp/pci084](https://doi.org/10.1093/pcp/pci084)
- Forti G, Furia A, Bombelli P, Finazzi G (2003) In vivo changes of the oxidation-reduction state of NADP and of the ATP/ADP cellular ratio linked to the photosynthetic activity in *Chlamydomonas reinhardtii*. *Plant Physiol* 132:1464–1474. doi:[10.1104/pp.102.018861](https://doi.org/10.1104/pp.102.018861)
- Foyer CH, Lelandais M, Harbinson J (1992) Control of the quantum efficiencies of photosystems I and II, electron flow, and enzyme activation following dark-to-light transitions in pea leaves. Relationship between NADP/NADPH ratios and NADP-Malate dehydrogenase activation state. *Plant Physiol* 99:979–986
- Genty B, Briantais JM, Baker N (1989) The relationship between the quantum yield of photosynthetic electron transport and quenching of chlorophyll fluorescence. *Biochim Biophys Acta* 990:87–92
- Golbeck JH, Cornelius JM (1986) Photosystem I charge separation in the absence of centres A and B. I. Optical characterization of centre A2 and evidence for its association with a 64 kDa peptide. *Biochim Biophys Acta* 849:16–24. doi:[10.1016/0005-2728\(86\)90091-5](https://doi.org/10.1016/0005-2728(86)90091-5)
- Golding AJ, Johnson GN (2003) Down-regulation of linear and activation of cyclic electron transport during drought. *Planta* 218:107–114. doi:[10.1007/s00425-003-1077-5](https://doi.org/10.1007/s00425-003-1077-5)
- Hampp R, Goller M, Füllgraf H (1984) Determination of compartmented metabolite pools by a combination of rapid fractionation of oat mesophyll protoplasts and enzymatic cycling. *Plant Physiol* 75:1017–1021
- Harbinson J, Hedley CL (1989) The kinetics of P-700⁺ reduction in leaves: a novel in situ probe of thylakoid functioning. *Plant Cell Environ* 12:357–369. doi:[10.1111/j.1365-3040.1989.tb01952.x](https://doi.org/10.1111/j.1365-3040.1989.tb01952.x)
- Harbinson J, Hedley CL (1993) Changes in P-700 oxidation during the early stages of the induction of photosynthesis. *Plant Physiol* 103:649–660
- Harbinson J, Genty B, Foyer C (1990) Relationship between photosynthetic electron transport and stromal enzyme activity in pea leaves. Toward an understanding of the nature of photosynthetic control. *Plant Physiol* 94:545–553
- Hashimoto M, Endo T, Peltier G, Tasaka M, Shikanai T (2003) A nucleus-encoded factor, CRR2, is essential for the expression of chloroplast *ndhB* in *Arabidopsis*. *Plant J* 36:541–549. doi:[10.1046/j.1365-3113X.2003.01900.x](https://doi.org/10.1046/j.1365-3113X.2003.01900.x)
- Heineke D, Riens B, Grosse H, Hoferichter P, Peter U, Flügge UI et al (1991) Redox transfer across the inner chloroplast envelope membrane. *Plant Physiol* 95:1131–1137
- Hiyama T (1985) Quantum yield and requirement for photo-oxidation of P700. *Physiol Veg* 23:605–610
- Hiyama T, Ke B (1971) A further study of P-430: a possible primary electron acceptor of photosystem I. *Arch Biochem Biophys* 147:99–108. doi:[10.1016/0003-9861\(71\)90314-6](https://doi.org/10.1016/0003-9861(71)90314-6)
- Holtgreffe S, Bader KP, Horton P, Scheibe R, von Schaewen A, Backhausen JE (2003) Decreased content of leaf ferredoxin changes electron distribution and limits photosynthesis in transgenic potato plants. *Plant Physiol* 133:1768–1778. doi:[10.1104/pp.103.026013](https://doi.org/10.1104/pp.103.026013)
- Johnson GN (2005) Cyclic electron transport in C₃ plants: fact or artifact? *J Exp Bot* 56:407–416. doi:[10.1093/jxb/eri106](https://doi.org/10.1093/jxb/eri106)
- Joliot P, Joliot A (2002) Cyclic electron transfer in plant leaf. *Proc Natl Acad Sci USA* 99:10209–10214. doi:[10.1073/pnas.102306999](https://doi.org/10.1073/pnas.102306999)
- Joliot P, Joliot A (2005) Quantification of cyclic and linear flows in plants. *Proc Natl Acad Sci USA* 102:4913–4918. doi:[10.1073/pnas.0501268102](https://doi.org/10.1073/pnas.0501268102)
- Joliot P, Béal D, Joliot A (2004) Cyclic electron flow under saturating excitation of dark-adapted *Arabidopsis* leaves. *Biochim Biophys Acta* 1656:166–176. doi:[10.1016/j.bbabi.2004.03.010](https://doi.org/10.1016/j.bbabi.2004.03.010)
- Kirchhoff H, Schöttler MA, Maurer J, Weis E (2004) Plastocyanin redox kinetics in spinach chloroplasts: evidence for disequilibrium in the high potential chain. *Biochim Biophys Acta* 1659:63–72. doi:[10.1016/j.bbabi.2004.08.004](https://doi.org/10.1016/j.bbabi.2004.08.004)
- Klughammer C, Schreiber U (1991) Analysis of light-induced absorbance changes in the near-infrared spectral region. I. Characterization of various components in isolated chloroplasts. *Z Naturforsch* 46:233–244
- Klughammer C, Schreiber U (1994) An improved method, using saturating light pulses, for the determination of photosystem I quantum yield via P700⁺-absorbance changes at 830 nm. *Planta* 192:261–268. doi:[10.1007/BF01089043](https://doi.org/10.1007/BF01089043)
- Laisk A, Siebke K, Gerst U, Eichelmann H, Oja V, Heber U (1991) Oscillations in photosynthesis are initiated and supported by imbalances in the supply of ATP and NADPH to the Calvin cycle. *Planta* 185:554–562. doi:[10.1007/BF00202966](https://doi.org/10.1007/BF00202966)

- Laisk A, Eichelmann H, Oja V, Peterson RB (2005) Control of cytochrome b_6/f at low and high light intensity and cyclic electron transport in leaves. *Biochim Biophys Acta* 1708:79–90. doi: [10.1016/j.bbabi.2005.01.007](https://doi.org/10.1016/j.bbabi.2005.01.007)
- Nikolaeva MK (2001) Activation of ferredoxin-NADP⁺ oxidoreductase in *Vicia faba* leaves induced by a short-term increase in irradiance. *Russ J Plant Physiol* 48:601–607. doi: [10.1023/A:1016799701081](https://doi.org/10.1023/A:1016799701081)
- Nuijs AM, Shuvalov VA, Van Gorkom HJ, Plijter JJ, Duysens LNM (1986) Picosecond absorbance difference spectroscopy on the primary reactions and the antenna excited states in photosystem I particles. *Biochim Biophys Acta* 850:310–318. doi: [10.1016/0005-2728\(86\)90186-6](https://doi.org/10.1016/0005-2728(86)90186-6)
- Oja V, Eichelmann H, Peterson RB, Rasulov B, Laisk A (2003) Deciphering the 820 nm signal: redox state of donor side and quantum yield of photosystem I in leaves. *Photosynth Res* 78: 1–15. doi: [10.1023/A:1026070612022](https://doi.org/10.1023/A:1026070612022)
- Rebeille F, Hatch MD (1986) Regulation of NADP-Malate dehydrogenase in C₄ plants: relationship among enzyme activity, NADPH to NADP ratios, and thioredoxin redox states in intact maize mesophyll chloroplasts. *Arch Biochem Biophys* 249: 171–179. doi: [10.1016/0003-9861\(86\)90572-2](https://doi.org/10.1016/0003-9861(86)90572-2)
- Rumeau D, Bécuwe-Linka N, Beyly A, Louwagie M, Garin J, Peltier G (2005) New subunits NDH-M, -N, and -O, encoded by nuclear genes, are essential for plastid Ndh complex functioning in higher plants. *Plant J* 17:219–232
- Sage RF (1990) A model describing the regulation of ribulose-1, 5-bisphosphate carboxylase, electron transport and triose phosphate use in response to light intensity and CO₂ in C₃ plants. *Plant Physiol* 94:1728–1734
- Shikanai T (2007) Cyclic electron transport around photosystem I: genetic approaches. *Annu Rev Plant Biol* 58:199–217. doi: [10.1146/annurev.arplant.58.091406.110525](https://doi.org/10.1146/annurev.arplant.58.091406.110525)
- Shinkarev VP, Zybilov B, Vassiliev IR, Golbeck JH (2002) Modeling of the P700⁺ charge recombination kinetics with phyloquinone and plastoquinone in the A₁ site of photosystem I. *Biophys J* 83:2885–2897
- Siebke K, von Caemmerer S, Badger M, Furbank R (1997) Expressing an *RbcS* antisense gene in transgenic *Flaveria bidentis* leads to an increased quantum requirement for CO₂ fixed in photosystem I and II. *Plant Physiol* 115:1163–1174
- Sonoike K, Terashima I, Iwaki M, Itoh S (1995) Destruction of photosystem I iron-sulfur centers in leaves of *Cucumis sativus* L. by weak illumination at chilling temperatures. *FEBS Lett* 362: 235–238. doi: [10.1016/0014-5793\(95\)00254-7](https://doi.org/10.1016/0014-5793(95)00254-7)
- Takahama U, Shimizu-Takahama M, Heber U (1981) The redox state of the NADP system in illuminated chloroplasts. *Biochim Biophys Acta* 637:530–539. doi: [10.1016/0005-2728\(81\)90060-8](https://doi.org/10.1016/0005-2728(81)90060-8)
- Takahashi Y, Katoh S (1984) Triplet states in a photosystem I reaction center complex. Inhibition of radical pair recombination by bipyridinium dyes and naphthoquinones. *Plant Cell Physiol* 25:785–794
- Talts E, Oja V, Rämme H, Rasulov B, Anijalg A, Laisk A (2007) Dark inactivation of ferredoxin-NADP reductase and cyclic electron flow under far-red light in sunflower leaves. *Photosynth Res* 94:109–120. doi: [10.1007/s11120-007-9224-7](https://doi.org/10.1007/s11120-007-9224-7)
- Usuda H (1988) Adenine nucleotide levels, the redox state of the NADP system, and assimilatory force in nonaqueously purified mesophyll chloroplasts from maize leaves under different light intensities. *Plant Physiol* 88:1461–1468